Reducing Planetary Health Risks Through Short-Lived Climate Forcer Mitigation

Yiqi Zheng[1] and Nadine Unger[2]

[1]Geophysical Institute, University of Alaska Fairbanks, Fairbanks, AL, USA, [2]Jiangsu Key Laboratory of Atmospheric Environment Monitoring and Pollution Control, Collaborative Innovation Center of Atmospheric Environment and Equipment Technology, School of Environmental Science and Engineering, Nanjing University of Information Science Technology, Nanjing, China

Abstract Global air pollution and climate change are major threats to planetary health. These threats are strongly linked through the short-lived climate forcers (SLCFs); ozone (O_3), aerosols, and methane (CH_4). Understanding the impacts of ambitious SLCF mitigation in different source emission sectors on planetary health indicators can help prioritize international air pollution control strategies. A global Earth system model is applied to quantify the impacts of idealized 50% sustained reductions in year 2005 emissions in the eight largest global anthropogenic source sectors on the SLCFs and three indicators of planetary health: global mean surface air temperature change (ΔGSAT), avoided $PM_{2.5}$-related premature mortalities and gross primary productivity (GPP). The model represents fully coupled atmospheric chemistry, aerosols, land ecosystems and climate, and includes dynamic CH_4. Avoided global warming is modest, with largest impacts from 50% cuts in domestic (−0.085 K), agriculture (−0.034 K), and waste/landfill (−0.033 K). The 50% cuts in energy, domestic, and agriculture sector emissions offer the largest opportunities to mitigate global $PM_{2.5}$-related health risk at around 5%–7% each. Such small global impacts underline the challenges ahead in achieving the World Health Organization aspirational goal of a 2/3 reduction in the number of deaths from air pollution by 2030. Uncertainty due to natural climate variability in $PM_{2.5}$ is an important underplayed dimension in global health risk assessment that can vastly exceed uncertainty due to the concentration-response functions at the large regional scale. Globally, cuts to agriculture and domestic sector emissions are the most attractive targets to achieve climate and health co-benefits through SLCF mitigation.

Plain Language Summary Climate mitigation action must be taken immediately on a global scale if we are to stay within the Paris Agreement temperature limit of well below 2°C. In addition to damaging human and global forest health, air pollutants influence global climate change, some cause global warming, and others cause global cooling. Reducing global air pollution can advance multiple United Nations Sustainable Development Goals but the actual environmental impacts of targeted mitigation options are not well understood. When there are many mitigation options to choose from, with limited resources, decisions must be made to prioritise one action over another and ensure win-win solutions for both climate and heath. This study uses an Earth system model to calculate the impacts of deep cuts in air pollutant emissions from different economic sources sectors on global temperature, human health and land ecosystem health.

1. Introduction

Aerosols, ozone (O_3), and methane (CH_4) have important impacts on global climate change but shorter atmospheric lifetimes than carbon dioxide (CO_2) ranging from days to months for aerosols and O_3 and up to about a decade for CH_4 (Myhre et al., 2013). These species are collectively referred to as the short-lived climate forcers (SLCFs). Sulfate, nitrate, and organic carbon aerosol are predominantly cooling whereas CH_4, O_3, and black carbon aerosol are predominantly warming (Boucher et al., 2013; Myhre et al., 2013). Their shorter atmospheric lifetimes confer the mitigation advantage that reductions in emissions or atmospheric formation of the SLCFs can rapidly alter the radiative forcing of global climate change (UNEP & WMO, 2011).

Writing – original draft: Yiqi Zheng, Nadine Unger
Writing – review & editing: Yiqi Zheng, Nadine Unger

Aerosols and O_3 are also toxic air pollutants that influence surface air quality with impacts on human and land ecosystem health (Feng et al., 2021; Jerrett et al., 2009; Pope & Dockery, 2006; Wittig et al., 2009; Yue & Unger, 2014). Exposure to ambient outdoor air pollution is the leading environmental health risk factor globally estimated to cause over 4 million premature mortalities every year worldwide, predominantly from aerosol particulates less than ≤2.5 μm in diameter known as $PM_{2.5}$ (Cohen et al., 2017). $PM_{2.5}$ is composed of different aerosol types including sulfate, nitrate, black carbon, organic carbon and dust. The World Health Organization (WHO) has set an aspirational goal to reduce the number of deaths from air pollution, including those associated with outdoor $PM_{2.5}$ exposure, by 2/3 by 2030 (WHO, 2018). Surface O_3 damages land ecosystem health by causing cellular impairment inside leaves, reducing photosynthetic rates, plant production, and growth with consequences for carbon sequestration and crop yields (Ainsworth et al., 2012).

There is a consensus that reductions in SLCFs play a critical role in advancing multiple United Nations Sustainable Development Goals (Haines et al., 2017; Rogelj et al., 2018; Shindell et al., 2017). However, there is much less agreement on the actual environmental impacts of targeted SLCF mitigation (Rogelj et al., 2018). For instance, there is a large spread in the published estimates of the contribution of SLCFs to global climate change mitigation ranging from an estimate of 0.5 K of avoided warming over the next 25 years to no impact on medium- and long-term climate targets (Lelieveld et al., 2019; Rogelj et al., 2015; S. J. Smith & Mizrahi, 2013; Stohl et al., 2015; Strefler et al., 2014; UNEP & WMO, 2011).

Assessment of mitigation impacts by economic source sector is a valuable method to determine the efficacy of individually controlling sources, for example, through fuel switching or increasing energy efficiency, and therefore to help identify priority mitigation measures that tackle a range of different pollutants and activities. Several studies have attributed air pollution-related premature mortalities to specific emission source sectors (Conibear et al., 2018; Lelieveld et al., 2015; Reddington et al., 2019; Silva et al., 2016). Typically, the previous assessments of human health impacts by source sector have not calculated the simultaneous climate and/or land ecosystem impacts. Similarly, assessments of the global climate impacts of SLCFs by source emission sector have not considered the air quality and human health impacts (Fuglestvedt et al., 2008; Lund et al., 2020; Unger et al., 2010). A few studies do assess both the climate and health effects of various specific activities and/or mitigation strategies (Huang et al., 2020; Kapadia et al., 2016; Shindell et al., 2012; Sofiev et al., 2018). These previous global human health impact studies have tended to provide results for a single year of air pollutant emissions only, neglecting interannual meteorological variability that may be an important dimension of uncertainty in global health risk assessment (Saari et al., 2019). Moreover, previous sector-based health assessments have not represented interactive CH_4 atmospheric concentrations, either ignoring the CH_4 response of the associated emission change or calculating the CH_4 response off-line using simplified metrics. CH_4 is of particular importance in linking air quality and climate change issues. CH_4 oxidation is a major source of background O_3 (Fiore et al., 2008). Through atmospheric lifetime dependence on the hydroxyl radical (OH), CH_4 is linked interactively to O_3 precursors and secondary aerosol components of $PM_{2.5}$ that depend upon oxidation for atmospheric formation (Shindell et al., 2009). A comprehensive multi-year assessment is needed of both climate and health effects of SLCF mitigation by source sector. Because emission reductions of aerosols and $PM_{2.5}$ can lead to climate warming for some sectors, integrated climate change and air quality policies that specifically target co-beneficial solutions are essential to ensure win-win and avoid unintended consequences (Schmale et al., 2014).

Newly available global earth system models that fully couple the chemistry-aerosol-land ecosystem-climate system capture the complexity of the interactions and allow the integrated prediction of multiple environmental impacts in response to SLCF sector emission reduction mitigation options. Here, we apply the NASA ModelE2-YIBs global earth system model to quantify the impacts of sustained idealized 50% air pollutant emission reductions in eight global economic sectors on air quality and human health, global temperature, and land ecosystem health simultaneously. The model framework allows the simulation of multiple decades of output years facilitating assessment of uncertainties due to interannual climate variability. The planetary health indicators assessed in this study in response to the 50% air pollutant emission controls by source sector are: avoided $PM_{2.5}$-related premature mortality, global mean surface air temperature (ΔGSAT) and gross primary productivity (GPP). For the first time, this sector-based atmospheric impact study includes an interactive simulation of atmospheric CH_4 concentration and represents dynamic interactions between CH_4 and air pollutant emissions through changing atmospheric oxidation capacity (Harper et al., 2018). The

eight global source sectors are: agriculture (AGR), agricultural waste burning (AWB), domestic (DOM), energy (ENE), industry (IND), transportation (TRA), waste/landfill (WST), and shipping (SHP). A companion study has detailed the impacts on land ecosystem health and GPP (Unger et al., 2020). Here, those results are presented within the context of the human health and ΔGSAT impacts.

2. Methods

2.1. Global Earth System Model

The global Earth system model framework is the NASA ModelE2 global chemistry-climate model (Schmidt et al., 2014) coupled to the Yale Interactive Terrestrial Biosphere Model (YIBs) (Yue & Unger, 2015). This study applies 2° × 2.5° latitude by longitude horizontal resolution with 40-vertical layers extending to 0.1 hPa. The atmospheric chemistry, aerosols and land ecosystems interact with each other and the physics of the climate model. The troposphere and stratosphere are coupled in terms of both dynamics and chemistry (Shindell et al., 2013). NASA ModelE2-YIBs incorporates a dynamic CH_4 simulation in which atmospheric CH_4 concentration is chemically interactive with atmospheric oxidation capacity (Harper et al., 2018). The model configuration simulates rapid adjustments in the climate system by allowing O_3, CH_4, and aerosols to affect the model radiation and, therefore, meteorology and dynamics. The vegetation is described using eight ecosystem types: tundra, C3 grassland, C4 grassland, shrubland, deciduous broadleaf forest, evergreen needleleaf forest, tropical rainforest, and C3 cropland. The satellite-derived global vegetation cover data set is from the Community Land Model that is based on retrievals from both the Moderate Resolution Imaging Spectroradiometer and the Advanced Very High Resolution Radiometer (Oleson et al., 2010). The atmospheric composition and land ecosystem fluxes have been well documented and extensively compared with observations and other models through several on-going multi-model international assessments (e.g., Bowman et al., 2013; Harper et al., 2018; Samset et al., 2014; Stevenson et al., 2013; Yue & Unger, 2015; Yue et al., 2017).

2.2. Simulations

A control simulation is performed (CTRL) representing the climatological period 2003–2007. Prescribed monthly varying sea ice concentrations and sea surface temperatures for the 2003–2007 average are derived from the global observation-based Hadley Centre Sea Ice and Sea Surface Temperature data set (Rayner et al., 2006). Global anthropogenic emissions of short-lived precursors and CH_4 for year 2005 are from the Greenhouse gas-Air pollution Interactions and Synergies integrated assessment model (Amann et al., 2011) (http://gains.iiasa.ac.at) except for aviation, international shipping, and biomass burning that are taken from the RCP8.5 inventory (Riahi et al., 2011) (Table S1). A set of eight mitigation simulations are performed based on CTRL in which all air pollutant precursors (NO_x, CO, NMVOCs, CH_4, SO_2, NH_3, black carbon, organic carbon) from eight anthropogenic source sectors are reduced by 50% (Table 1). The mitigation simulations are labeled by the source sector that has been halved in the model run: AGR, AWB, DOM, ENE, IND, TRA, WST, SHP. Prescribed global annual mean surface-level mixing ratios of the non-CH_4 well-mixed greenhouse gases are from the RCP8.5 scenario (Riahi et al., 2011): 379.3 ppmv CO_2, 319.4 ppbv N_2O, and 793 pptv chlorofluorocarbons (CFCs = CFC-11 + CFC-12). All simulations are run for 30 years. Results are presented in terms of annual averages at the 20-year time scale that are the decadal average of model output years 15–24. The planetary health impacts due to the 50% source sector emission reductions are determined by taking the difference between the 50% mitigation simulation and CTRL (e.g., AGR–CTRL). The standard deviation of the $n = 10$ output years 15–24 is quantified to provide an assessment of uncertainty and is applied to determine statistical significance ($p < 0.05$) of the planetary health impact relative to interannual climate variability.

2.3. Calculation of Human Health Impacts

The model framework includes a mass-based aerosol scheme where aerosols are treated as externally mixed and have prescribed size and properties (Koch et al., 2007), including sea salt that has two distinct size classes and dust that has four size classes (Miller et al., 2006) and can be coated by sulfate and nitrate aerosols (Bauer et al., 2007). Dust classes include the clay category with particles with radii less than 1 μm, while

Table 1
Applied 50% Reductions in Global Anthropogenic Short-Lived Precursor Emissions From IIASA GAINS ECLIPSE v5a Emissions Inventory for Year 2005 (Amann et al., 2011; http://gains.iiasa.ac.at)

Sector	CO	NO_x	NMVOC	CH_4	SO_2	NH_3	BC	OC
AGR	0	0.345	0	62.1	0	23.17	0	0
AWB	13.6	0.045	2.1	1.65	0.085	0.325	0.165	0.64
DOM	110.6	0.805	15.95	6.95	4.015	0.185	1.99	4.2
ENE	4.6	3.915	8.25	64.4	29.1	0.02	0.28	0.24
IND	46.35	2.805	1.2	0.85	15.98	0.22	0.195	0.175
SHP	0.65	2.865	1.55	0.25	6.52	0	0.07	0.075
TRA	96.35	6.935	13.15	1.3	1.14	0.325	0.745	0.665
WST	3.1	0.02	0.7	23.95	0.03	1.545	0.05	0.375

Note. Units are Tg/yr full molecular mass except for NO_x (TgN/yr).

Abbreviations: AGR, agriculture; AWB, agricultural waste burning; DOM, domestic; ENE, energy; GAINS, Greenhouse gas-Air pollution Interactions and Synergies; IND, industry; SHP, shipping; TRA, transportation; WST, waste/landfill.

the three silt classes have radii between 1–2, 2–4, and 4–8 µm, respectively (Miller et al., 2006). Sea salt size classes include a submicrometer one with dry effective radius of 0.44 µm, and a supermicrometer one with dry effective radius of 1.7 µm (Schmidt et al., 2014). Here, $PM_{2.5}$ is defined as the sum of sulfate, nitrate, black carbon, organic carbon (primary and secondary), clay, the 1–2 µm size class of silt and both sea salt size classes.

Several dose-response functions have been developed to assess the premature mortality due to $PM_{2.5}$ exposure (e.g., Burnett et al., 2014, 2018; Krewski et al., 2009). Here, we apply an integrated exposure response (IER) model that has been previously used in global-scale assessments of human health effects caused by specific emission sources (Anenberg et al., 2017; Huang et al., 2020; Morita et al., 2014) and was applied in the Global Burden of Disease Assessment 2015 (Cohen et al., 2017). The IER model uses information from alternative particulate exposures, including active and second hand smoking, to determine the flattening shape of the dose-response curve at high $PM_{2.5}$ concentrations (Burnett et al., 2014). Five specific health endpoints that contribute to $PM_{2.5}$-related premature mortality are assessed including children's (<5 years) acute lower respiratory infection (ALRI); adult (>25 years) chronic obstructive pulmonary disease (COPD), lung cancer (LC), ischemic heart disease (IHD), and stroke. For each global model grid cell (i, j) and health endpoint, the relative risk ($RR_{i,j,h}$) of $PM_{2.5}$-related premature mortality takes the following form:

$$RR_{i,j,h} = 1 + \alpha \left[1 - e^{\left(-\gamma \left(C_{i,j} - C_0 \right)^{\beta} \right)} \right] \tag{1}$$

where $C_{i,j}$ is the annual mean $PM_{2.5}$ concentration; C_0 is the minimum threshold $PM_{2.5}$ concentration below which the exposure does not pose any excess risk, C_0 is assumed to be 5.8 µg m⁻³ in this study, the minimum concentration from the IER model cohorts (Lim et al., 2012); central, low, and high values of α, γ, and β parameters for IHD, stroke, LC, and COPD are from a statistical fitting of the concentration-response functions (Burnett et al., 2014; Morita et al., 2014) where the low and high bounds represent the 95% confidence interval (CI). RR for ALRI is from a precalculated lookup table (Apte et al., 2015).

Premature mortality ($M_{i,j,h}$) in each grid cell (i, j) and for each health endpoint (h) is given by:

$$M_{i,j,h} = POP_{i,j} \times BMR_{i,j,h} \times \left[\frac{RR_{i,j,h} - 1}{RR_{i,j,h}} \right] \tag{2}$$

$POP_{i,j}$ is the population density in each grid cell from the Center for International Earth Science Information Network Gridded Population of the World version 4 (GPWv4) data set for year 2005; $BMR_{i,j,h}$ is the

baseline mortality rate in each grid cell for each health endpoint Institute for Health Metrics and Evaluation (http://ghdx.healthdata.org/gbd-results-tool). BMRs for each health endpoint were extracted for the 11 regions of the Global Burden of Disease Assessment (GBD 2015 Risk Factors Collaborators, 2016) defined in Figure S1. $PM_{2.5}$-related premature mortality is determined by summing across all five health endpoints for each of the 11 regions and globally (the sum of all 11 regions). Calculations are performed for $PM_{2.5}$ surface concentrations from CTRL and the eight mitigation simulations that reduce air pollution emissions from each source sector by 50%. The avoided $PM_{2.5}$-related premature mortalities due to the 50% source sector emission reductions are determined by taking the difference between the 50% mitigation simulation and CTRL (e.g., AGR–CTRL). The avoided $PM_{2.5}$-related premature mortalities are calculated for central, low and high values of the RR parameters (Morita et al., 2014). The calculations are performed for all 30 model output years. Avoided $PM_{2.5}$-related premature mortalities are presented at the 20-year time scale and for the integrated total at 20 years since mitigation. The 20-year time scale results are the decadal average of model output years 15–24. The standard deviation of those $n = 10$ years of avoided $PM_{2.5}$-related premature mortalities for central, low and high RR cases is quantified that provides an assessment of uncertainty due to interannual climate variability and is applied to determine statistical significance ($p < 0.05$) of the avoided mortalities relative to interannual climate variability.

2.4. Calculation of Effective Radiative Forcing

Effective radiative forcing (ERF) is the change in net top of the atmosphere (TOA) downward radiative flux after allowing for atmospheric and land temperatures, water vapor and clouds to adjust. ERF is calculated by fixing sea surface temperatures (SSTs) and sea ice cover at climatological values while allowing all other parts of the system (land-atmosphere) to respond until reaching steady state. The global earth system model computes ERFs of CH_4, O_3, sulfate, nitrate, black carbon, primary organic carbon, and secondary organic aerosol at TOA (at the tropopause for O_3). The model does not include the short-wave ERF for CH_4 (Etminan et al., 2016). The CH_4-induced stratospheric water vapor response is estimated as 15% of the CH_4 ERF (Myhre et al., 2007). ERFs due to aerosol-cloud interactions induced by the 50% sector air pollutant emission reductions are estimated using scalings of the aerosol-radiation interactions output from the model (Bond et al., 2013).

2.5. Calculation of GSAT Impacts

The GSAT responses to the 50% emission sector reductions are calculated by implementing the time-dependent (for 30 years) ERFs for all species or the net ERF into the Finite Amplitude Impulse Response (FAIR) simple climate model version 1.4 (Millar et al., 2017; Smith et al., 2018). The FAIR model reasonably reproduces the climate behavior shown in complex earth system models (Millar et al., 2017; Smith et al., 2018). This approach allows for a more realistic simulation of GSAT temporal evolution than has been done in previous sector studies because it represents the coupled model transient methane and atmospheric composition system responses.

2.6. Calculation of Land Ecosystem Health Impacts

NASA ModelE2-YIBs includes a flux-based O_3 damage scheme that allows plant carbon assimilation and stomatal conductance to respond to on-line simulated atmospheric O_3 concentration (Yue & Unger, 2014; Yue et al., 2017). The change in GPP due to O_3 damage is calculated as the linear average of the low- and high-O_3 plant sensitivity parameter cases. The model is designed to internally diagnose three forms of GPP: (a) GPP_0 that only responds to changes in physical climate; (b) GPP_{High} that also responds to O_3 damage assuming high O_3 plant sensitivity; (c) GPP_{Low} that also responds to O_3 damage assuming low O_3 plant sensitivity. For each simulation, the O_3 damage on GPP is calculated as:

$$\Delta GPP_{O_3} = 0.5 \times \left[\left(GPP_{High} - GPP_0 \right) + \left(GPP_{Low} - GPP_0 \right) \right] \tag{3}$$
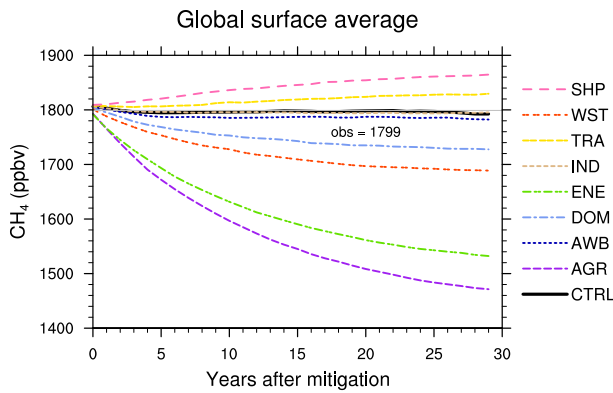
Figure 1. Response of global average surface methane (CH_4) concentration in ppbv to the 50% air pollutant emission reductions by source sector. AGR, agriculture; AWB, agricultural waste burning; DOM, domestic; ENE, energy; IND, industry; SHP, shipping; TRA, transportation; WST, waste/landfill.

ΔGPP due to the 50% source sector emission reductions is calculated as the difference in GPP_{O_3} for the mitigation simulation and CTRL. A detailed description of the GPP impact results is provided in a companion study (Unger et al., 2020).

3. Results

### 3.1. Impacts on Atmospheric CH_4 Concentration

In CTRL, the global area-weighted surface average CH_4 is 1,796 ppbv (Northern Hemisphere [NH] = 1,844 ppbv; Southern Hemisphere [SH] = 1,748 ppbv) compared to the observed value of 1,799 ppbv for year 2005 (NH = 1,843 ppbv; SH = 1,754 ppbv) (Dlugokencky et al., 2015). The CH_4 concentration responses to the 50% sector mitigation experiments are shown in Figure 1. The CH_4 atmospheric concentrations on the 20-year time scale after mitigation are shown in Table 2. The sectors can be split into 2 groups, those with a substantial CH_4 emission (AGR, ENE, WST, DOM, AWB) and those without substantial CH_4 emission (IND, TRA, SHP). All sectors emit other air pollutants that influence the CH_4 lifetime. Reduction of sector emissions by 50% decreases CH_4 concentrations from AGR, ENE, WST, DOM, and AWB but increases CH_4 concentrations from TRA and SHP with little net impact for IND. Large 20-year time scale atmospheric CH_4 concentration decreases occur for AGR (−310 ppbv), ENE (−232 ppbv), WST (−98 ppbv), and DOM (−60 ppbv). There is variability in CH_4 e-folding response time between sectors (in years): AGR = 12.9; ENE = 12.4; WST = 11.4; DOM = 10.3. This variability is due to the different combinations of air pollutant co-emissions from the sectors, especially NO_x and

Table 2
Impacts on Planetary Health Indicators of the 50% Air Pollutant Emission Reductions by Source Sector on the 20-Year Time Scale

Sector	CH_4 conc (ppbv)	Avoided $PM_{2.5}$ mortalities (×1,000 persons)	Integrated $PM_{2.5}$ avoided mortalities at 20 years since mitigation (×1,000 persons)	ΔERF (mWm^{-2})	ΔGSAT (mK)	ΔGPP (TgC/yr)
AGR	1,514 ± 19	154 (80, 227)	3,374 (1,761, 4,942)	−119 ± 33	−34 ± 13	324 ± 173
AWB	1,787 ± 1	*31 (18, 45)*	656 (329, 1,018)	−25 ± 21	−8 ± 3	N/A
		p = 0.06				
DOM	1,736 ± 3	166 (89, 245)	3,267 (1,739, 4,817)	−206 ± 22	−85 ± 5	234 ± 191
ENE	1,566 ± 15	218 (115, 324)	3,963 (2,094, 5,912)	−22 ± 33	0.2 ± 8	502 ± 194
IND	1,794 ± 1	77 (38, 120)	1,786 (874, 2,720)	+94 ± 31	+41 ± 3	280 ± 168
SHP	1,854 ± 5	*16 (9, 27)*	566 (331, 827)	+46 ± 36	+21 ± 4	133 ± 203
		p = 0.19				
TRA	1,823 ± 3	89 (44, 139)	2,118 (1,079, 3,232)	−42 ± 24	−17 ± 3	754 ± 237
WST	1,699 ± 6	*8 (3, 14)*	466 (233, 708)	−79 ± 30	−33 ± 2	152 ± 141
		p = 0.35				

Notes. Values of one standard deviation due to interannual climate variability are indicated with ± ranges. Values in parentheses for avoided $PM_{2.5}$ mortalities are uncertainty bounds determined from the 95% CI for low and high RR parameters. Values for one standard deviation due to interannual climate variability for the avoided $PM_{2.5}$ mortalities are shown in the Tables S3–S5. Results that are not statistically robust ($p < 0.05$) relative to interannual climate variability are shown in italics with the *p*-value. The integrated $PM_{2.5}$ avoided mortalities are calculated over the sum of model runs years 1–20. ΔGPP values are from Unger et al. (2020) (ΔGPP results for AWB were negligible and therefore not analyzed).

Abbreviations: AGR, agriculture; AWB, agricultural waste burning; DOM, domestic; ENE, energy; ERF, effective radiative forcing; GSAT, global mean surface air temperature change; GPP, gross primary productivity; IND, industry; RR, relative risk; SHP, shipping; TRA, transportation; WST, waste/landfill.
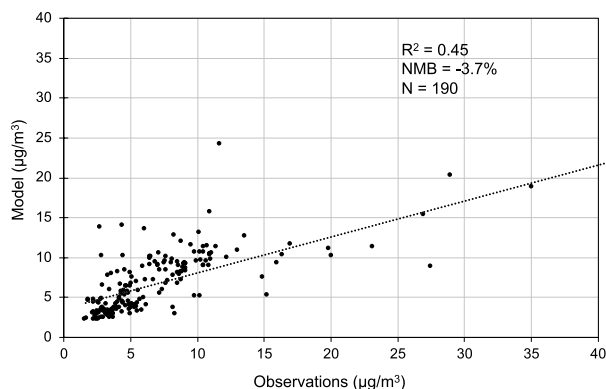
Figure 2. Comparison of annual average modeled and observational surface $PM_{2.5}$ concentrations (in $\mu g/m^3$) for the 2000s climatological period at 190 sites worldwide from three monitoring networks in The Global Aerosol Synthesis and Science Project GASSP: (IMPROVE, APAD, EMEP) (Reddington et al., 2017).

CO. These pollutants influence OH levels and the oxidation capacity and feedback to the CH_4 lifetime in opposite ways, in addition to the OH-regulated positive feedback of CH_4 on its own lifetime. Halving emissions from TRA and SHP results in increased CH_4 concentrations (Figure 1, Table 2). These sectors are substantial emitters of NO_x. Removal of the NO_x emissions decreases OH and oxidation capacity leading to an increase in CH_4 lifetime and an accumulation of CH_4 in the atmosphere from other sources.

3.2. Evaluation of Surface $PM_{2.5}$

Annual average model surface $PM_{2.5}$ for the 2000s climatological period from CTRL (Figure S2) is evaluated against $PM_{2.5}$ observations from The Global Aerosol Synthesis and Science Project (GASSP) (Reddington et al., 2017) (Figure 2). The GASSP database includes long-term measurements from over 350 ground-based monitoring stations spanning 1990–2015 predominantly in North America, Europe and East Asia from the IMPROVE, EMEP, and APAD networks. The observational annual average 2000s surface $PM_{2.5}$ climatology is derived using sites that have 12 full months of annual data for a minimum of 5 individual years between 2000 and 2009 comprising 190 sites. The model annual average 2000s climatology is calculated using the 30 model output years of the control simulation. The model data was extracted at site co-ordinates using linear interpolation. Here, the model surface $PM_{2.5}$ performs reasonably well against the monitored surface $PM_{2.5}$ observations with a correlation coefficient (R^2) of 0.45 and normalized mean bias of -3.7%. The model tends to overpredict observed concentrations around the 5–10 $\mu g/m^3$ range and underpredict higher observed values around the 20–30 $\mu g/m^3$ range consistent with a previous evaluation of multiple global models (Turnock et al., 2020).

3.3. Impacts on Human Health

Figure 3 shows the spatial distribution of the total global $PM_{2.5}$-related premature mortalities in CTRL. Table S2 presents the global and regional $PM_{2.5}$-related premature mortalities in CTRL for the central, low and high RR cases and includes one standard deviation due to interannual climate variability for $n = 10$ model output years. The global health burden risk from $PM_{2.5}$ mortalities is 2.975 million persons (Table S2). The largest regional contributions are from China (34%), India (16%), Rest of Asia (16%), Eastern and Central Europe (9%), North Africa and Middle East (8%), and Sub-Saharan Africa (7%). Western Europe has more than double the health burden of USA (6% vs. 2.5%).

Figure 4 shows the spatial distribution of the total avoided global $PM_{2.5}$-related premature mortalities for the 50% sector mitigation experiments including statistical significance ($p < 0.05$) relative to interannual climate variability (also summarized in Table 2). Tables S3–S5 show the avoided global and regional $PM_{2.5}$ mortalities due to the 50% sector mitigation relative to CTRL for the central, low, and high RR cases for the 20-year time scale. The avoided $PM_{2.5}$ premature mortalities for each region, sector emission reduction and RR (central, low, high) case include the standard deviation due to interannual climate variability for $n = 10$ model output years centered on the 20-year time scale since mitigation. Globally, under 50% emission reduction controls, ENE has the largest human health benefits offering 0.218 million avoided mortalities per year on the 20-year time scale. The next most important sectors are DOM (0.166 million per year), AGR (0.154 million per year), TRA (0.089 million per year), and IND (0.077 million per year) (Table 2; Table S3). Integrated avoided mortalities 20 years since mitigation follow the same rankings as for the 20-year time scale results. Global cuts of 50% in source sector emissions from SHP, WST, and AWB do not have statistically significant ($p < 0.05$) impacts on avoided $PM_{2.5}$-related mortalities relative to interannual climate variability. However, their integrated impacts on avoided mortalities 20 years after the mitigation together reach up to 1.7 million persons. At the global-scale, 50% reductions of emissions from the AGR, DOM, ENE, IND, and TRA source sectors mitigates the risk to the global human health burden by 5.2%, 5.6%, 7.3%, 2.6%, and 3.0%, respectively.

TOT_mortality / 1000
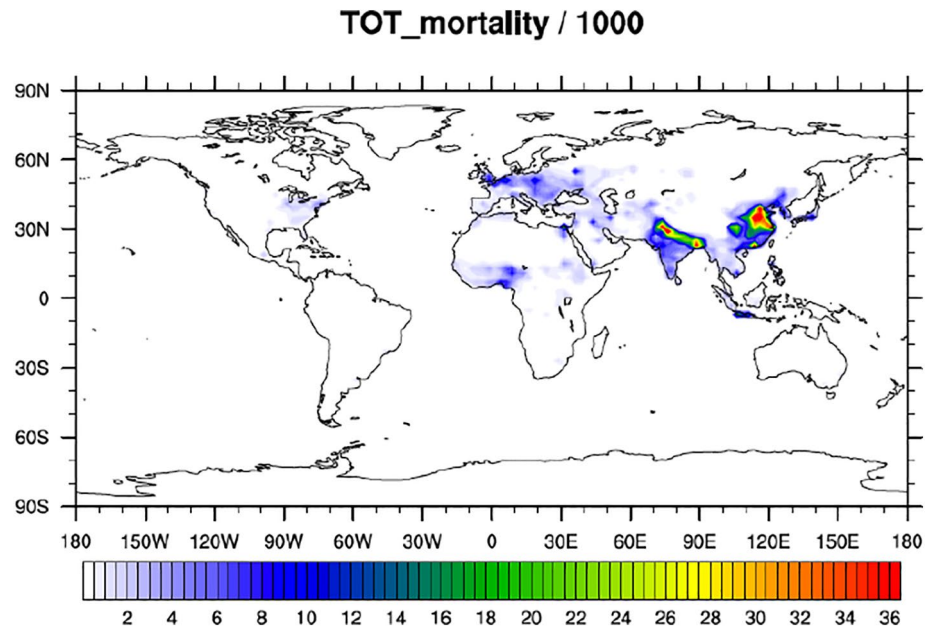
Figure 3. Spatial distribution of the total $PM_{2.5}$-related premature mortality in CTRL in units of persons ($\times 1 \times 10^{-3}$) including five health endpoints including acute lower respiratory infection (<5 years); adult (>25 years) chronic obstructive pulmonary disease, lung cancer, ischemic heart disease, and stroke. Results are the decadal average from $PM_{2.5}$ model output years 15–24.

For the global-scale human health impacts of the 50% sector mitigation, the one standard deviation due to interannual climate variability is of comparable magnitude but is generally less than the 95% CI due to the low and high RR cases (Table 2, Tables S3–S5). However, at the regional-scale, one standard deviation due to interannual climate variability can be much larger than the 95% CI due to the low and high RR cases (Tables S3–S5). Thus, the human health impacts of 50% reductions in air pollutant emissions by source sector in the GBD regions are in many cases not statistically robust ($p < 0.05$) relative to interannual climate variability (Figure 4). In China, the 50% reductions in ENE have the largest human health benefit with avoided premature mortalities of 79,000 per year (Tables S3–S6). DOM (68,000 per year), AGR (46,000 per year), IND (42,000 per year), and TRA (18,000 per year) are also important in China. The 50% sector reductions in DOM have the largest benefits to human health in India (30,000 per year), Latin America (3,000 per year) and Sub-Saharan Africa (11,000 per year). Remarkably, in Western Europe, Eastern and Central Europe, USA, and Canada, AGR has the largest health benefit with annual mean avoided deaths of 22,000 per year, 51,000 per year, 21,000 per year, and 2,000 per year, respectively (Tables S3–S6). Mitigation of ENE and TRA emissions are also important in those regions.

Figure 5 shows the fraction of the $PM_{2.5}$-attributable premature mortalities in the major GBD world regions that are mitigated by the 50% emission cuts in global source sectors. Differences between regions reflect different regional source portfolios, different natural source contributions, different annual average total $PM_{2.5}$ concentrations and the nonlinear flattening shape of concentration-response functions at high $PM_{2.5}$. For the regions that contribute the largest to the global burden of $PM_{2.5}$-related deaths, China, India and Rest of Asia, 50% cuts in ENE and DOM emissions offer at most 6%–7% improvements in the $PM_{2.5}$-attributable premature mortalities. Fifty percentage cuts in IND and TRA mitigate the human health risk by less than 5% in those regions. AGR is important in China but not in India or Rest of Asia. Opportunities for mitigation of $PM_{2.5}$-attributable premature mortalities are higher in USA, Western Europe, Eastern and Central Europe, and Latin America. In USA, 50% cuts in emissions from AGR can mitigate 25% of the $PM_{2.5}$-attributable premature mortalities. Fifty percentage cuts in ENE and TRA mitigate about 15% of the $PM_{2.5}$-related premature mortality burden in USA. $PM_{2.5}$-attributable mortalities can be mitigated by about 12% from the 50% emission cuts in AGR, ENE and TRA in Western Europe and by over 15% from the 50% emission cuts in AGR and ENE in Eastern and Central Europe.

Avoided Mortality / 1000 (ctrl-sect)
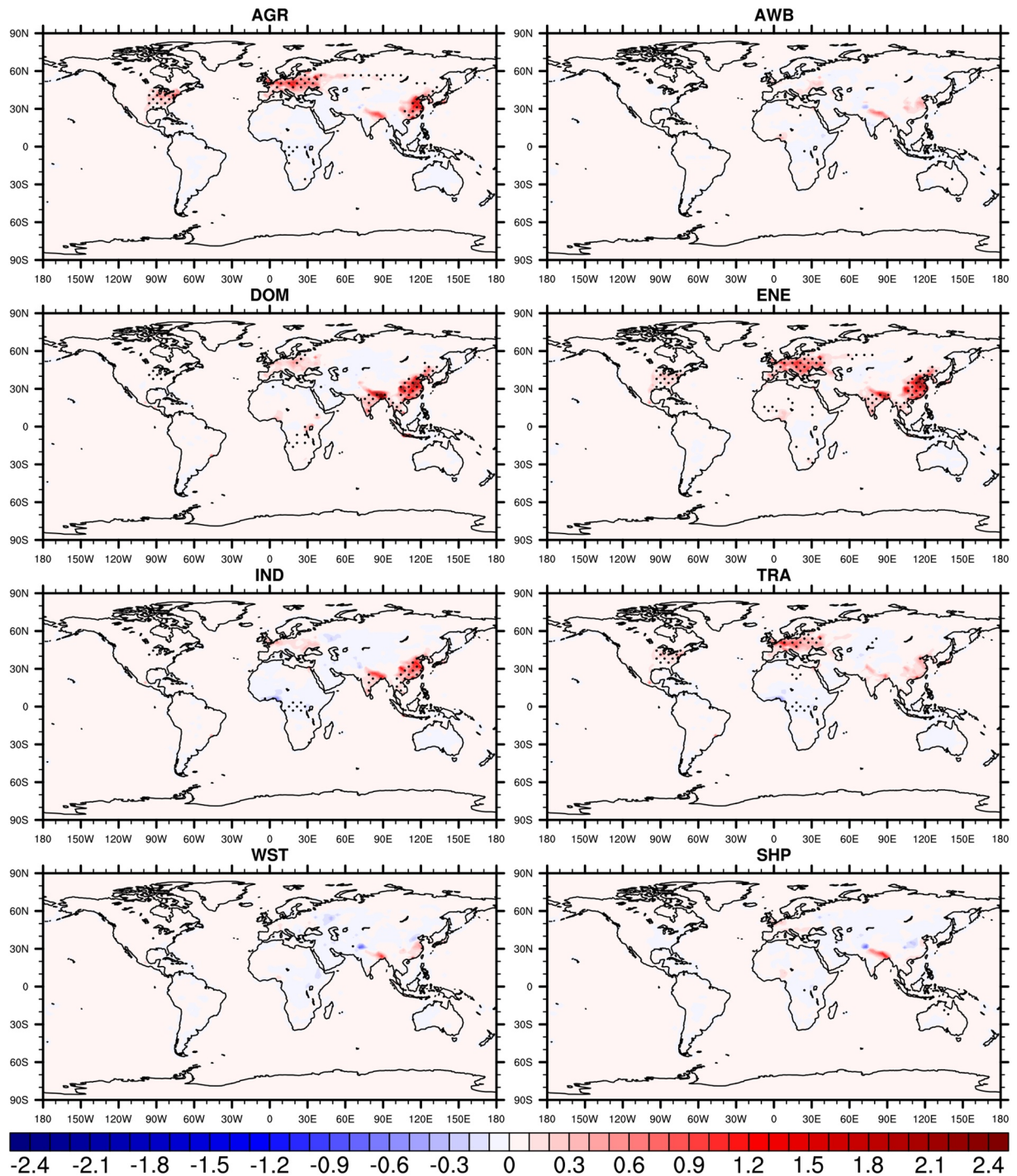
Figure 4. Avoided PM$_{2.5}$-related premature mortalities due to the 50% sector mitigation experiments in units of persons ($\times 1 \times 10^{-3}$). Results are the decadal average from model output years 15–24 for the central value of relative risk parameters. Statistically significant avoided mortalities relative to interannual climate variability ($p < 0.05$) are marked with black dots. AGR, agriculture; AWB, agricultural waste burning; DOM, domestic; ENE, energy; IND, industry; SHP, shipping; TRA, transportation; WST, waste/landfill.
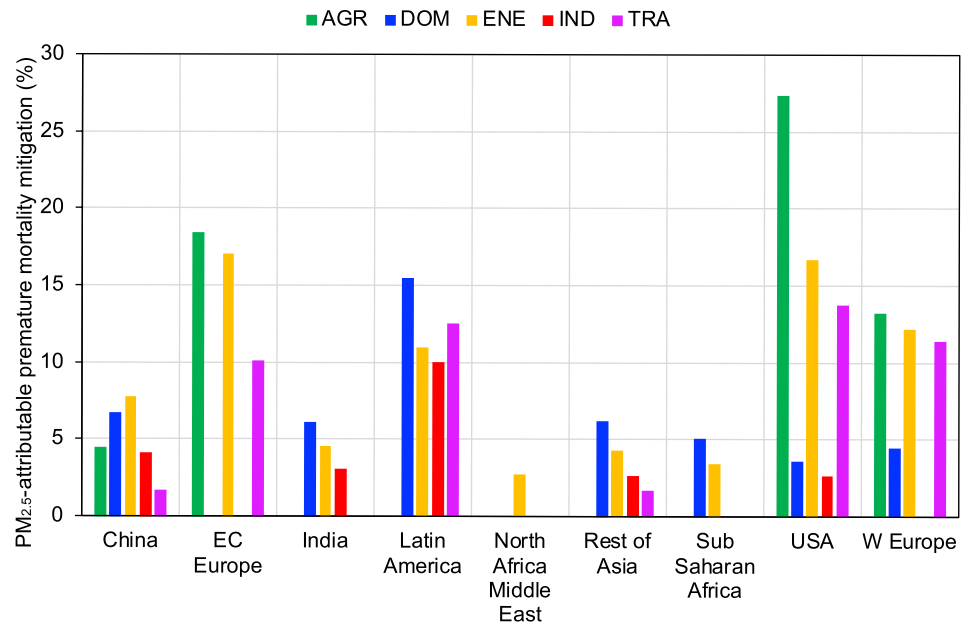
Figure 5. Fraction of total PM$_{2.5}$-attributable premature mortalities in the major Global Burden of Disease Assessment world regions that are mitigated by the 50% emission cuts in global source sectors (%). Results are on the 20-year time scale since the emission reduction. AGR, agriculture; DOM, domestic; ENE, energy; IND, industry; TRA, transportation.

3.4. Impacts on ERF

The 20-year time scale net ΔERFs in response to the 50% emission sector reductions are presented in Figure 6 and Table 2. Figure S3 shows the time evolution of the ΔERFs for the sustained emission sector mitigation including results by individual species. Halving emissions from the DOM and AGR sectors have the largest net negative 20-year ΔERFs, but for different reasons. The ΔERF of −206 mWm^{-2} for DOM is dominated by reduced black carbon with O$_3$ and CH$_4$ reductions of secondary importance. Halving emissions from the AGR sector has the largest single net negative CH$_4$ ΔERF with associated negative ΔERF contributions from decreased O$_3$ and stratospheric H$_2$O. However, the large net negative ΔERF for AGR is substantially offset by the warming induced by nitrate aerosol decrease such that the 50% emission reductions in AGR lead to a moderated net negative 20-year ERF of −119 mWm^{-2}. In addition, the increased atmospheric oxidation capacity from the AGR CH$_4$ reductions drives production of sulfate aerosol that together with associated aerosol-cloud impacts contributes to a small negative ERF. Halving emissions from ENE has the second largest negative CH$_4$ ΔERF, and the strongest negative O$_3$ ΔERF amongst all sectors. For ENE, the net negative ΔERFs from CH$_4$ and O$_3$ and smaller contributions from black carbon, nitrate aerosol and stratospheric H$_2$O are largely offset by the large net positive ΔERF driven by reduced sulfate and cloud effects, resulting in the smallest net negative 20-year ΔERF amongst all sectors of about −22 mWm^{-2}. Fifty percentage cuts in emissions from WST has a net negative 20-year ΔERF of −79 mWm^{-2} dominated by CH$_4$ reduction; 50% cuts in emissions from ΔTRA has a smaller net negative 20-year ERF of −42 mWm^{-2} dominated by decreases in black carbon and O$_3$; 50% cuts in emissions from AWB has a small net negative ΔERF of −25 mWm^{-2} dominated by black carbon reductions. Halving emissions from SHP and IND results in net positive ΔERFs of 46 and 94 mWm^{-2}, respectively. The net positive ΔERF for IND is dominated by reductions in sulfate and associated cloud effects. While sulfate and cloud play an important role in the net positive ΔERF for SHP, the overall response is dominated by increased atmospheric CH$_4$ following reductions in NO$_x$ and atmospheric oxidation capacity from this sector.

3.5. Impacts on GSAT

The 20-year time scale net global ΔGSAT responses to the 50% sector mitigation experiments are shown in Figure 6 and Table 2. Figure S4 shows the time evolution of the ΔGSAT for the sustained emission sector
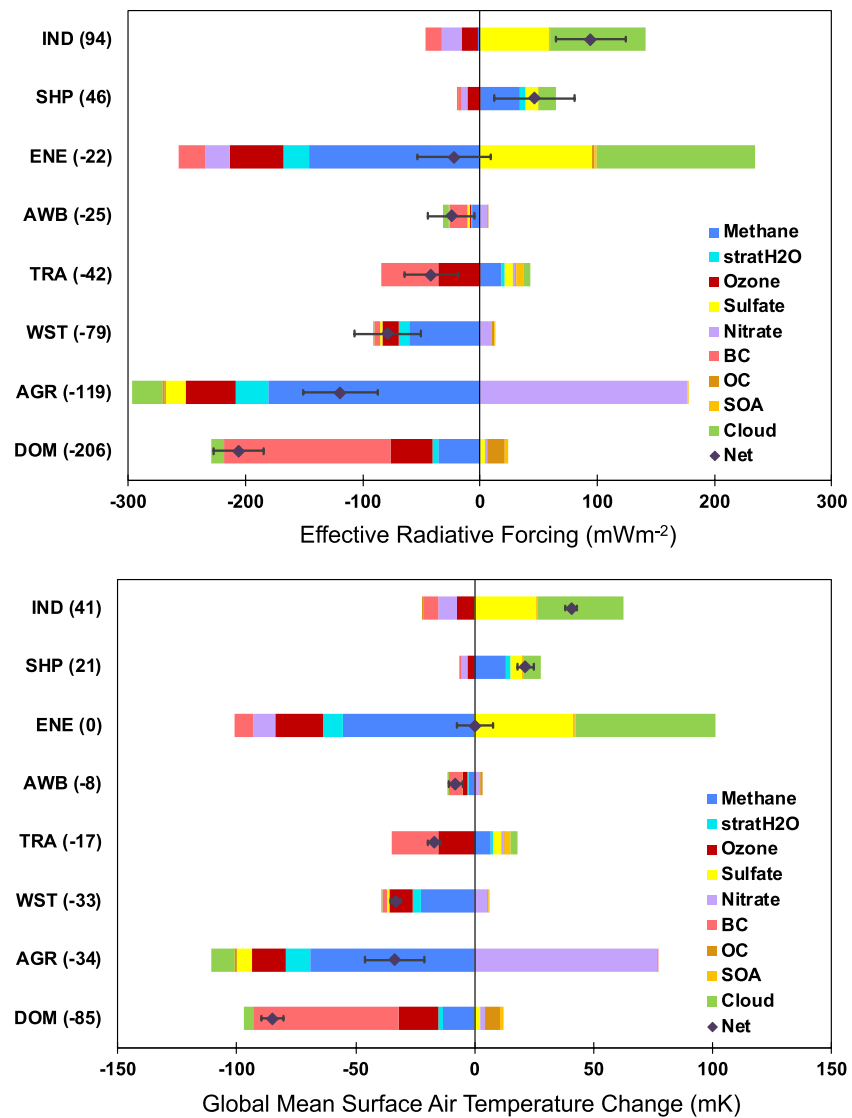
Figure 6. Global impacts of 50% air pollutant emission reductions by source sector on 20-year time scale effective radiative forcings (ΔERFs) in mWm^{-2} (top panel) and global mean surface air temperature change (ΔGSAT) in mK (bottom panel). The net value is shown with diamond symbol. The uncertainty ranges represent one standard deviation calculated from model output years 15–24 $n = 10$ based on interannual climate variability. AGR, agriculture; AWB, agricultural waste burning; BC, black carbon; Cloud, aerosol-cloud interactions; DOM, domestic; ENE, energy; IND, industry; OC, organic carbon; SHP, shipping; stratH2O, stratospheric water vapor; SOA, secondary organic aerosol; TRA, transportation; WST, waste/landfill.

mitigation including results by individual species and the net value for each sector. The global ΔGSAT response rankings follow the ΔERF results. For AGR and ENE, ΔGSAT increases in the first few years due to rapid warming driven by aerosol reductions (nitrate for AGR, and sulfate and associated cloud effects for ENE). After about a decade, ΔGSAT begins to decrease due to the cooling driven by the CH$_4$ reductions in these sectors. Consequently, the 20-year ΔGSATs for AGR (−0.034 K) and ENE (0.0002 K) are substantially smaller than for DOM (−0.085 K). For other sectors, ΔGSAT is nearly monodirectional (Figure S4). The ΔGSAT responses reach steady-state for most sectors after the 20-year time scale (Figure S4), except for AGR, which is associated with the largest CH$_4$ change. Mitigation in DOM, AGR and WST sectors offer the largest global cooling benefits, with ΔGSAT of −0.085 K, −0.034 K, and −0.033 K, respectively. IND mitigation shows the largest global warming response, with ΔGSAT of +0.041 K on the 20-year time scale. Net ΔGSAT has a linear relationship with input net ΔERF at the 20-year time scale of 0.39 K/(Wm^{-2})
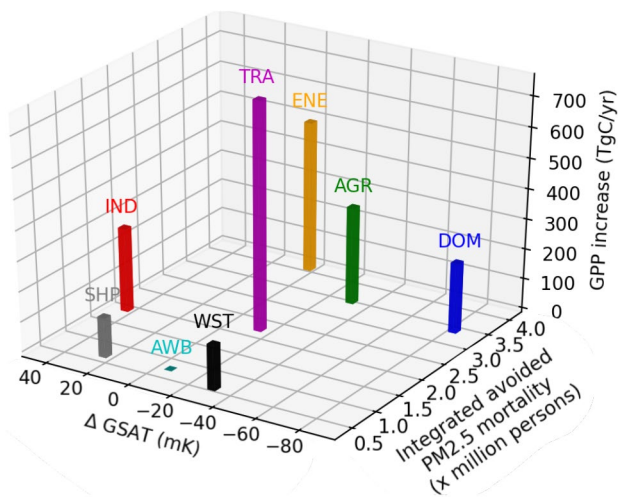
Figure 7. Combined global impacts of 50% air pollutant emission reductions by source sector on 20-year time scale global mean surface air temperature (ΔGSAT, mK), integrated avoided PM$_{2.5}$-related premature mortalities (×1,000 persons) and 20-year time scale ΔGPP (TgC/yr). AGR, agriculture; AWB, agricultural waste burning; DOM, domestic; ENE, energy; GPP, gross primary productivity; IND, industry; SHP, shipping; TRA, transportation; WST, waste/landfill.

($R^2 = 0.97$) (Figure S5) that offers a convenient simple metric for determining ΔGSAT from net ΔERFs of SLCF changes.

3.6. Integrated Framework for Planetary Health

Figure 7 provides an integrated perspective of the impacts of 50% mitigation of air pollutant emissions by source sector on planetary health. Global reductions in air pollutant emissions from ENE, AGR, and DOM offer the largest human health benefits by avoiding PM$_{2.5}$-induced premature mortality whereas global reductions in TRA and ENE offer the largest benefits to GPP recovery from reduced O$_3$ exposure. The largest benefits to global cooling are from the 50% source sector reductions in DOM, followed by AGR and WST. The 50% emission cuts in IND and SHP result in enhanced global warming. From the global perspective, emission reductions in DOM and AGR are the most attractive options offering the largest integrated benefits to global climate and health. In developed countries such as USA and Western Europe, emissions reductions in AGR and TRA offer the largest impact for co-beneficial global climate and health solutions. In China, India and developing countries, emissions reductions in DOM stand out as having the largest impact for co-beneficial global climate and health solutions. ENE emissions are a major contributor to human and ecosystem health impacts in both developed and developing regions and ENE emissions must be reduced to protect planetary health and achieve the UN sustainable development goals. However, reduction of ENE emissions will have little impact on global temperature through SLCF mitigation due to offsetting warming and cooling effects. Achieving planetary health benefits from SLCF mitigation requires ambitious mitigation pathways that tackle multiple source sectors.

4. Discussion and Conclusions

A fully coupled global Earth system model has been applied to quantify the impacts of idealized 50% reductions in year 2005 emissions by source sector on the SLCFs and associated planetary health impacts. Priority measures for international SLCF mitigation depend on the underlying motivation of the policy. If the motivation is to protect global climate, priority measures are reductions in the domestic, agriculture and waste/landfill sectors. If the motivation is to protect global air quality and human and ecosystem health, then priority measures are reductions in the energy, agriculture, domestic, and transportation sectors. Globally, mitigation of domestic and agriculture sector emissions stand out as unambiguously most beneficial to both climate and health simultaneously.

Our results are in qualitative agreement with previous sector-based health impact studies, for instance, studies agree on the geographical distribution of PM$_{2.5}$ health impacts by sector, the importance of the domestic sector in India and China and the importance of agricultural and transportation emissions in developed regions (Lelieveld et al., 2015; Reddington et al., 2019; Silva et al., 2016). However, using the IER model in this work, halving emissions from the energy sector results in the largest avoided PM$_{2.5}$-related premature mortalities globally, whereas previous studies attribute the largest overall global PM$_{2.5}$ health impacts to the domestic sector (Lelieveld et al., 2015; Silva et al., 2016). Such different health impact results between global studies are driven by differences in the methodological approach (50% emission reductions vs. zero-out attribution methods), differences in concentration-response functions, emissions, sector definitions, PM$_{2.5}$ simulations, and the availability of modeled fine mode aerosol components to include in PM$_{2.5}$.

In particular, application of the supra-linear IER dose-response function gives different quantitative results for the attribution of premature mortality to source emission sector versus the impact of removing emissions from specific source sectors, especially in highly polluted regions such as India and China (Apte et al., 2015; Conibear et al., 2018; Reddington et al., 2019). A previous study based on the IER model showed that mitigation of the global health burden is challenging because substantial decreases in risk burden in

highly polluted regions like India and China require drastic reductions in concentration, and, for a given reduction in $PM_{2.5}$ concentration, reductions in per-capita mortality is higher in cleaner locales (Apte et al., 2015).

We suggest that the important role of interannual climate variability has been underplayed in previous global-scale human health impact assessments that have typically performed analyses based on a single year of model $PM_{2.5}$ output from a global chemical-transport model. Application of a single year of model $PM_{2.5}$ data masks uncertainty due to interannual climate variability, an important dimension of uncertainty in global health risk assessment that can vastly exceed uncertainties due to the concentration-response functions at the large regional scale. For example, cutting emissions globally by 50% in the shipping, agricultural waste burning and waste/landfill sectors do not have statistically robust impacts on avoided $PM_{2.5}$-attributable premature mortalities at the 95% confidence level. In other words, the reductions in $PM_{2.5}$ induced by halving the emissions from those sectors are not particularly important compared to meteorologically driven year-to-year changes in $PM_{2.5}$ concentrations in the emission regions. Shipping has received substantial attention in the sector-based health impacts community in part because of the new fuel-sulfur cap implemented by the International Maritime Organization on January 1, 2020 (Bilsback et al., 2020; Partanen et al., 2013; Sofiev et al., 2018; Winebrake et al., 2009).

The study has several limitations. The human health results presented here depend on the selection of the IER concentration-response model. The newly updated Global Exposure Mortality Model (GEMM) based only on cohort studies of outdoor air pollution that covers the global exposure range no longer has a flattening supra-linear shape at high $PM_{2.5}$ but a linear or super-linear shape that yields much larger premature deaths due to $PM_{2.5}$ exposure than using the IER model (Bilsback et al., 2020; Burnett et al., 2018). For example, application of GEMM to fractional selective emissions reduction health impact calculations would lead to enhanced benefits in high $PM_{2.5}$ concentration regions such as China and India relative to the IER model. Our analysis is based on year 2005 anthropogenic emissions. SLCF emissions have changed substantially between 2005 and the present day, most notably through reductions in BC and aerosol precursors and increases in CH_4 (Hoesly et al., 2018). Updated present day emissions will show enhanced global climate benefits of emission reductions from CH_4 dominated sectors relative to the year 2005 results shown here. The human health and ecosystem health results may be particularly sensitive to the model's horizontal grid resolution (e.g., Punger & West, 2013). This study has not assessed the health impacts of other air pollutants such as O_3 (Anenberg et al., 2017) and heat (Shindell et al., 2020). This study estimated aerosol-cloud interactions based on scalings of the model's aerosol-radiation interactions (Bond et al., 2013). There are large uncertainties in aerosol-cloud interactions that influence the ERF and global temperature change calculations and have not been systematically assessed here (Boucher et al., 2013).

The integrated holistic approach presented here is useful because it is independent of the underlying motivation of the emission reductions, air quality and/or climate. This approach can be used to guide climate and health informed decisions of emission sector reductions. Emissions reductions in agriculture, agricultural waste burning, domestic, transportation, and waste/landfill all have net cooling impacts on global climate through the SLCFs. Integrated co-beneficial solutions for global climate and health can be most effectively achieved through targeting emissions reductions in the agriculture and transportation sectors in developed countries and through targeting emissions reductions in the domestic sector in China, India and developing countries. The modest 5%–7% reductions in $PM_{2.5}$-attributable premature mortality achieved through aggressive 50% emissions cuts in individual source sectors emphasize the challenges involved in realizing the WHO aspirational goal of mitigating the global air pollution health burden by 2/3 by 2030. In future research, the framework can be expanded to include more planetary health indicators, for example, the effects of reactive nitrogen deposition to the biosphere, O_3 impacts on human health and heat-related human health effects.

Conflict of Interest

The authors declare no conflicts of interest relevant to this study.

Data Availability Statement

The NASA ModelE2-YIBs surface PM$_{2.5}$ concentration data sets for the control and mitigation experiments have been archived at https://figshare.com/s/6aa231a7ab68607b12aa (doi placeholder https://doi.org/10.6084/m9.figshare.13373828). The baseline mortality rates data are publicly available at IHME (http://ghdx.healthdata.org/gbd-results-tool).

References

Ainsworth, E. A., Yendrek, C. R., Sitch, S., Collins, W. J., & Emberson, L. D. (2012). The effects of tropospheric ozone on net primary productivity and implications for climate change. *Annual Review of Plant Biology*, *63*(1), 637–661. https://doi.org/10.1146/annurev-arplant-042110-103829

Amann, M., Bertok, I., Borken-Kleefeld, J., Cofala, J., Heyes, C., Höglund-Isaksson, L., et al. (2011). Cost-effective control of air quality and greenhouse gases in Europe: Modeling and policy applications. *Environmental Modelling & Software*, *26*(12), 1489–1501. https://doi.org/10.1016/j.envsoft.2011.07.012

Anenberg, S. C., Miller, J., Minjares, R., Du, L., Henze, D. K., Lacey, F., et al. (2017). Impacts and mitigation of excess diesel-related NOx emissions in 11 major vehicle markets. *Nature*, *545*(7655), 467–471. https://doi.org/10.1038/nature22086

Apte, J. S., Marshall, J. D., Cohen, A. J., & Brauer, M. (2015). Addressing global mortality from ambient PM2.5. *Environmental Science and Technology*, *49*(13), 8057–8066. https://doi.org/10.1021/acs.est.5b01236

Bauer, S. E., Mishchenko, M. I., Lacis, A. A., Zhang, S., Perlwitz, J., & Metzger, S. M. (2007). Do sulfate and nitrate coatings on mineral dust have important effects on radiative properties and climate modeling? *Journal of Geophysical Research*, *112*(D6), D06307. https://doi.org/10.1029/2005JD006977

Bilsback, K. R., Kerry, D., Croft, B., Ford, B., Jathar, S. H., Carter, E., et al. (2020). Beyond SO x reductions from shipping: Assessing the impact of NO x and carbonaceous-particle controls on human health and climate. *Environmental Research Letters*, *15*(12), 124046. https://doi.org/10.1088/1748-9326/abc718

Bond, T. C., Doherty, S. J., Fahey, D. W., Forster, P. M., Berntsen, T., Deangelo, B. J., et al. (2013). Bounding the role of black carbon in the climate system: A scientific assessment. *Journal of Geophysical Research: Atmospheres*, *118*(11). https://doi.org/10.1002/jgrd.50171

Boucher, O., Randall, D., Artaxo, P., Bretherton, C., Feingold, G., Forster, P., et al. (2013). Clouds and aerosols. In T. F. Stocker, D. Qin, G.-K. Plattner, M. Tignor, S. K. Allen, J. Boschung, et al. (Eds.), *Climate change 2013—The Physical Science Basis Working Group I Contribution to the Fifth Assessment Report of the Intergovernmental Panel on Climate Change* (Vol. 9781107057, pp. 571–657). Cambridge University Press. https://doi.org/10.1017/CBO9781107415324.008

Bowman, K. W., Shindell, D. T., Worden, H. M., Lamarque, J. F., Young, P. J., Stevenson, D. S., et al. (2013). Evaluation of ACCMIP outgoing longwave radiation from tropospheric ozone using TES satellite observations. *Atmospheric Chemistry and Physics*, *13*(8), 4057–4072. https://doi.org/10.5194/acp-13-4057-2013

Burnett, R. T., Arden Pope, C., Ezzati, M., Olives, C., Lim, S. S., Mehta, S., et al. (2014). An integrated risk function for estimating the global burden of disease attributable to ambient fine particulate matter exposure. *Environmental Health Perspectives*, *122*(4), 397–403. https://doi.org/10.1289/ehp.1307049

Burnett, R. T., Chen, H., Szyszkowicz, M., Fann, N., Hubbell, B., Pope, C. A., et al. (2018). Global estimates of mortality associated with long-term exposure to outdoor fine particulate matter. *Proceedings of the National Academy of Sciences of the United States of America*, *115*(38), 9592–9597. https://doi.org/10.1073/pnas.1803222115

Cohen, A. J., Brauer, M., Burnett, R., Anderson, H. R., Frostad, J., Estep, K., et al. (2017). Estimates and 25-year trends of the global burden of disease attributable to ambient air pollution: An analysis of data from the Global Burden of Diseases Study 2015. *The Lancet*, *389*(10082), 1907–1918. https://doi.org/10.1016/S0140-6736(17)30505-6

Conibear, L., Butt, E. W., Knote, C., Arnold, S. R., & Spracklen, D. V. (2018). Residential energy use emissions dominate health impacts from exposure to ambient particulate matter in India. *Nature Communications*, *9*(1), 617. https://doi.org/10.1038/s41467-018-02986-7

Dlugokencky, E. J., Lang, P. M., Crotwell, A. M., Masarie, K. A., & Crotwell, M. J. (2015). *Atmospheric methane dry air model fractions from the NOAA ESRL carbon cycle cooperative global air sampling network, 1983–2014, version 2015-08-03*. Retrieved from http://aftp.cmdl.noaa.gov/data/trace_gases/ch4/flask/surface/

Etminan, M., Myhre, G., Highwood, E. J., & Shine, K. P. (2016). Radiative forcing of carbon dioxide, methane, and nitrous oxide: A significant revision of the methane radiative forcing. *Geophysical Research Letters*, *43*(24), 12614–12623. https://doi.org/10.1002/2016GL071930

Feng, Z., Agathokleous, E., Yue, X., Oksanen, E., Paoletti, E., Sase, H., et al. (2021). Emerging challenges of ozone impacts on Asian plants: Actions are needed to protect ecosystem health. *Ecosystem Health and Sustainability*, *7*(1), 1911602. https://doi.org/10.1080/20964129.2021.1911602

Fiore, A. M., West, J. J., Horowitz, L. W., Naik, V., & Schwarzkopf, M. D. (2008). Characterizing the tropospheric ozone response to methane emission controls and the benefits to climate and air quality. *Journal of Geophysical Research*, *113*(D8), D08307. https://doi.org/10.1029/2007JD009162

Fuglestvedt, J., Berntsen, T., Myhre, G., Rypdal, K., & Skeie, R. B. (2008). Climate forcing from the transport sectors. *Proceedings of the National Academy of Sciences of the United States of America*, *105*(2), 454–458. https://doi.org/10.1073/pnas.0702958104

GBD 2015 Risk Factors Collaborators. (2016). Global, regional, and national comparative risk assessment of 79 behavioral, environmental and occupational, and metabolic risks or clusters of risks, 1990–2015: A systematic analysis for the Global Burden of Disease Study 2015. *The Lancet*, *388*(10053), 1659–1724. https://doi.org/10.1016/S0140-6736(16)31679-8

Haines, A., Amann, M., Borgford-Parnell, N., Leonard, S., Kuylenstierna, J., & Shindell, D. (2017). Short-lived climate pollutant mitigation and the Sustainable Development Goals. *Nature Climate Change*, *7*(12), 863–869. https://doi.org/10.1038/s41558-017-0012-x

Harper, K. L., Zheng, Y., & Unger, N. (2018). Advances in representing interactive methane in ModelE2-YIBs (version 1.1). *Geoscientific Model Development*, *11*(11), 4417–4434. https://doi.org/10.5194/gmd-11-4417-2018

Hoesly, R. M., Smith, S. J., Feng, L., Klimont, Z., Janssens-Maenhout, G., Pitkanen, T., et al. (2018). Historical (1750–2014) anthropogenic emissions of reactive gases and aerosols from the Community Emissions Data System (CEDS). *Geoscientific Model Development*, *11*(1), 369–408. https://doi.org/10.5194/gmd-11-369-2018

Huang, Y., Unger, N., Harper, K., & Heyes, C. (2020). Global climate and human health effects of the gasoline and diesel vehicle fleets. *GeoHealth*, *4*(3). https://doi.org/10.1029/2019GH000240

Jerrett, M., Burnett, R. T., Pope, C. A., Ito, K., Thurston, G., Krewski, D., et al. (2009). Long-term ozone exposure and mortality. *New England Journal of Medicine*, *360*(11), 1085–1095. https://doi.org/10.1056/NEJMoa0803894

Kapadia, Z. Z., Spracklen, D. V., Arnold, S. R., Borman, D. J., Mann, G. W., Pringle, K. J., et al. (2016). Impacts of aviation fuel sulfur content on climate and human health. *Atmospheric Chemistry and Physics*, *16*(16), 10521–10541. https://doi.org/10.5194/acp-16-10521-2016

Koch, D., Bond, T. C., Streets, D., Unger, N., & van der Werf, G. R. (2007). Global impacts of aerosols from particular source regions and sectors. *Journal of Geophysical Research*, *112*(D2), D02205. https://doi.org/10.1029/2005JD007024

Krewski, D., Jerrett, M., Burnett, R. T., Ma, R., Hughes, E., & Shi, Y. (2009). *Extended follow-up and spatial analysis of the American Cancer Society study linking particulate air pollution and mortality*.

Lelieveld, J., Evans, J. S., Fnais, M., Giannadaki, D., & Pozzer, A. (2015). The contribution of outdoor air pollution sources to premature mortality on a global scale. *Nature*, *525*(7569), 367–371. https://doi.org/10.1038/nature15371

Lelieveld, J., Klingmüller, K., Pozzer, A., Burnett, R. T., Haines, A., & Ramanathan, V. (2019). Effects of fossil fuel and total anthropogenic emission removal on public health and climate. *Proceedings of the National Academy of Sciences of the United States of America*, *116*(15), 7192–7197. https://doi.org/10.1073/pnas.1819989116

Lim, S. S., Vos, T., Flaxman, A. D., Danaei, G., Shibuya, K., Adair-Rohani, H., et al. (2012). A comparative risk assessment of burden of disease and injury attributable to 67 risk factors and risk factor clusters in 21 regions, 1990–2010: A systematic analysis for the Global Burden of Disease Study 2010. *The Lancet*, *380*(9859), 2224–2260. https://doi.org/10.1016/S0140-6736(12)61766-8

Lund, M. T., Aamaas, B., Stjern, C. W., Klimont, Z., Berntsen, T. K., & Samset, B. H. (2020). A continued role of short-lived climate forcers under the Shared Socioeconomic Pathways. *Earth System Dynamics*, *11*(4), 977–993. https://doi.org/10.5194/esd-11-977-2020

Millar, R. J., Nicholls, Z. R., Friedlingstein, P., & Allen, M. R. (2017). A modified impulse-response representation of the global near-surface air temperature and atmospheric concentration response to carbon dioxide emissions. *Atmospheric Chemistry and Physics*, *17*(11), 7213–7228. https://doi.org/10.5194/acp-17-7213-2017

Miller, R. L., Cakmur, R. V., Perlwitz, J., Geogdzhayev, I. V., Ginoux, P., Koch, D., et al. (2006). Mineral dust aerosols in the NASA Goddard Institute for Space Sciences ModelE atmospheric general circulation model. *Journal of Geophysical Research*, *111*(D6), D06208. https://doi.org/10.1029/2005JD005796

Morita, H., Yang, S., Unger, N., & Kinney, P. L. (2014). Global health impacts of future aviation emissions under alternative control scenarios. *Environmental Science & Technology*, *48*(24), 14659–14667. https://doi.org/10.1021/es5055379

Myhre, G., Nilsen, J. S., Gulstad, L., Shine, K. P., Rognerud, B., & Isaksen, I. S. A. (2007). Radiative forcing due to stratospheric water vapour from CH_4 oxidation. *Geophysical Research Letters*, *34*(1), L01807. https://doi.org/10.1029/2006GL027472

Myhre, G, Shindell, D. T., Breon, F, Collins, W, Fuglestvedt, J, Huang, J., et al. (2013). Anthropogenic and natural radiative forcing. In *Climate Change 2013: The Physical Science Basis*. Contribution of Working Group I to the Fifth Assessment Report of the Intergovernmental Panel on Climate Change.

Oleson, K. W., Lawrence, D. M., Bonan, G. B., Flanne, M. G., Kluzek, E., Lawrence, P. J., et al. (2010). *Technical description of version 4.0 of the Community Land Model (CLM)*.

Partanen, A. I., Laakso, A., Schmidt, A., Kokkola, H., Kuokkanen, T., Pietikäinen, J.-P., et al. (2013). Climate and air quality trade-offs in altering ship fuel sulfur content. *Atmospheric Chemistry and Physics*, *13*(23), 12059–12071. https://doi.org/10.5194/acp-13-12059-2013

Pope, C. A., & Dockery, D. W. (2006). Health effects of fine particulate air pollution: Lines that connect. *Journal of the Air & Waste Management Association*, *56*(6), 709–742. https://doi.org/10.1080/10473289.2006.10464485

Punger, E. M., & West, J. J. (2013). The effect of grid resolution on estimates of the burden of ozone and fine particulate matter on premature mortality in the USA. *Air Quality, Atmosphere & Health*, *6*(3), 563–573. https://doi.org/10.1007/s11869-013-0197-8

Rayner, N. A., Brohan, P., Parker, D. E., Folland, C. K., Kennedy, J. J., Vanicek, M., et al. (2006). Improved analyses of changes and uncertainties in sea surface temperature measured in situ since the mid-nineteenth century: The HadSST2 dataset. *Journal of Climate*, *19*(3), 446–469. https://doi.org/10.1175/JCLI3637.1

Reddington, C. L., Carslaw, K. S., Stier, P., Schutgens, N., Coe, H., Liu, D., et al. (2017). The global aerosol synthesis and science project (GASSP): Measurements and modeling to reduce uncertainty. *Bulletin of the American Meteorological Society*, *98*(9), 1857–1877. https://doi.org/10.1175/BAMS-D-15-00317.1

Reddington, C. L., Conibear, L., Knote, C., Silver, B. J., Li, Y. J., Chan, C. K., et al. (2019). Exploring the impacts of anthropogenic emission sectors on $PM_{2.5}$ and human health in South and East Asia. *Atmospheric Chemistry and Physics*, *19*(18), 11887–11910. https://doi.org/10.5194/acp-19-11887-2019

Riahi, K., Rao, S., Krey, V., Cho, C., Chirkov, V., Fischer, G., et al. (2011). RCP 8.5—A scenario of comparatively high greenhouse gas emissions. *Climatic Change*, *109*(1–2), 33–57. https://doi.org/10.1007/s10584-011-0149-y

Rogelj, J., Meinshausen, M., Schaeffer, M., Knutti, R., & Riahi, K. (2015). Impact of short-lived non-CO 2 mitigation on carbon budgets for stabilizing global warming. *Environmental Research Letters*, *10*(7), 075001. https://doi.org/10.1088/1748-9326/10/7/075001

Rogelj, J., Shindell, D., Jiang, K., Fifita, S., Forster, P., Ginzburg, V., et al. (2018). Mitigation pathways compatible with 1.5°C in the context of sustainable development. In Global warming of 1.5°C. An IPCC Special Report on the impacts of global warming of 1.5°C above pre-industrial levels and related global greenhouse gas emission pathways.

Saari, R. K., Mei, Y., Monier, E., & Garcia-Menendez, F. (2019). Effect of health-related uncertainty and natural variability on health impacts and cobenefits of climate policy. *Environmental Science & Technology*, *53*(3), 1098–1108. https://doi.org/10.1021/acs.est.8b05094

Samset, B. H., Myhre, G., Herber, A., Kondo, Y., Li, S.-M., Moteki, N., et al. (2014). Modelled black carbon radiative forcing and atmospheric lifetime in AeroCom Phase II constrained by aircraft observations. *Atmospheric Chemistry and Physics*, *14*(22), 12465–12477. https://doi.org/10.5194/acp-14-12465-2014

Schmale, J., van Aardenne, J., & von Schneidemesser, E. (2014). New directions: Support for integrated decision-making in air and climate policies—Development of a metrics-based information portal. *Atmospheric Environment*, *90*, 146–148. https://doi.org/10.1016/j.atmosenv.2014.03.016

Schmidt, G. A., Kelley, M., Nazarenko, L., Ruedy, R., Russell, G. L., Aleinov, I., et al. (2014). Configuration and assessment of the GISS ModelE2 contributions to the CMIP5 archive. *Journal of Advances in Modeling Earth Systems*, *6*(1), 141–184. https://doi.org/10.1002/2013MS000265

Shindell, D. T., Borgford-Parnell, N., Brauer, M., Haines, A., Kuylenstierna, J. C. I., Leonard, S. A., et al. (2017). A climate policy pathway for near- and long-term benefits. *Science*, *356*(6337), 493–494. https://doi.org/10.1126/science.aak9521

Shindell, D. T., Faluvegi, G., Koch, D., Schmidt, G., Unger, N., & Bauer, S. (2009). Improved attribution of climate forcing to emissions. *Science*, *326*(5953), 716–718. https://doi.org/10.1126/science.1174760

Shindell, D. T., Kuylenstierna, J. C. I., Vignati, E., van Dingenen, R., Amann, M., Klimont, Z., et al. (2012). Simultaneously mitigating near-term climate change and improving human health and food security. *Science*, *335*(6065), 183–189. https://doi.org/10.1126/science.1210026

Shindell, D. T., Pechony, O., Voulgarakis, A., Faluvegi, G., Nazarenko, L., Lamarque, J.-F., et al. (2013). Interactive ozone and methane chemistry in GISS-E2 historical and future climate simulations. *Atmospheric Chemistry and Physics*, *13*(5), 2653–2689. https://doi.org/10.5194/acp-13-2653-2013

Shindell, D. T., Zhang, Y., Scott, M., Ru, M., Stark, K., & Ebi, K. L. (2020). The effects of heat exposure on human mortality throughout the United States. *GeoHealth*, *4*(4). https://doi.org/10.1029/2019GH000234

Silva, R. A., Adelman, Z., Fry, M. M., & West, J. J. (2016). The impact of individual anthropogenic emissions sectors on the global burden of human mortality due to ambient air pollution. *Environmental Health Perspectives*, *124*(11), 1776–1784. https://doi.org/10.1289/EHP177

Smith, C. J., Forster, P. M., Allen, M., Leach, N., Millar, R. J., Passerello, G. A., & Regayre, L. A. (2018). FAIR v1.3: A simple emissions-based impulse response and carbon cycle model. *Geoscientific Model Development*, *11*(6), 2273–2297. https://doi.org/10.5194/gmd-11-2273-2018

Smith, S. J., & Mizrahi, A. (2013). Near-term climate mitigation by short-lived forcers. *Proceedings of the National Academy of Sciences of the United States of America*, *110*(35), 14202–14206. https://doi.org/10.1073/pnas.1308470110

Sofiev, M., Winebrake, J. J., Johansson, L., Carr, E. W., Prank, M., Soares, J., et al. (2018). Cleaner fuels for ships provide public health benefits with climate tradeoffs. *Nature Communications*, *9*(1), 406. https://doi.org/10.1038/s41467-017-02774-9

Stevenson, D. S., Young, P. J., Naik, V., Lamarque, J. F., Shindell, D. T., Voulgarakis, A., et al. (2013). Tropospheric ozone changes, radiative forcing and attribution to emissions in the Atmospheric Chemistry and Climate Model Intercomparison Project (ACCMIP). *Atmospheric Chemistry and Physics*, *13*(6), 3063–3085. https://doi.org/10.5194/Acp-13-3063-2013

Stohl, A., Aamaas, B., Amann, M., Baker, L. H., Bellouin, N., Berntsen, T. K., et al. (2015). Evaluating the climate and air quality impacts of short-lived pollutants. *Atmospheric Chemistry and Physics*, *15*(18), 10529–10566. https://doi.org/10.5194/acp-15-10529-2015

Strefler, J., Luderer, G., Kriegler, E., & Meinshausen, M. (2014). Can air pollutant controls change global warming? *Environmental Science & Policy*, *41*, 33–43. https://doi.org/10.1016/j.envsci.2014.04.009

Turnock, S. T., Allen, R. J., Andrews, M., Bauer, S. E., Deushi, M., Emmons, L., et al. (2020). Historical and future changes in air pollutants from CMIP6 models. *Atmospheric Chemistry and Physics*, *20*(23), 14547–14579. https://doi.org/10.5194/acp-20-14547-2020

UNEPWMO. (2011). *Integrated assessment of black carbon and tropospheric ozone. Summary for decision makers.*

Unger, N., Bond, T. C., Wang, J. S., Koch, D. M., Menon, S., Shindell, D. T., & Bauer, S. (2010). Attribution of climate forcing to economic sectors. *Proceedings of the National Academy of Sciences of the United States of America*, *107*(8), 3382–3387. https://doi.org/10.1073/pnas.0906548107

Unger, N., Zheng, Y., Yue, X., & Harper, K. L. (2020). Mitigation of ozone damage to the world's land ecosystems by source sector. *Nature Climate Change*, *10*(2), 134–137. https://doi.org/10.1038/s41558-019-0678-3

WHO. (2018). *First WHO global conference on air pollution and health—Summary report.*

Winebrake, J. J., Corbett, J. J., Green, E. H., Lauer, A., & Eyring, V. (2009). Mitigating the Health impacts of pollution from oceangoing shipping: An assessment of low-sulfur fuel mandates. *Environmental Science & Technology*, *43*(13), 4776–4782. https://doi.org/10.1021/es803224q

Wittig, V. E., Ainsworth, E. A., Naidu, S. L., Karnosky, D. F., & Long, S. P. (2009). Quantifying the impact of current and future tropospheric ozone on tree biomass, growth, physiology and biochemistry: A quantitative meta-analysis. *Global Change Biology*, *15*(2), 396–424. https://doi.org/10.1111/j.1365-2486.2008.01774.x

Yue, X., & Unger, N. (2014). Ozone vegetation damage effects on gross primary productivity in the United States. *Atmospheric Chemistry and Physics*, *14*(17). https://doi.org/10.5194/acp-14-9137-2014

Yue, X., & Unger, N. (2015). The Yale Interactive terrestrial Biosphere model version 1.0: Description, evaluation and implementation into NASA GISS ModelE2. *Geoscientific Model Development*, *8*(8), 2399–2417. https://doi.org/10.5194/gmd-8-2399-2015

Yue, X., Unger, N., Harper, K., Xia, X., Liao, H., Zhu, T., et al. (2017). Ozone and haze pollution weakens net primary productivity in China. *Atmospheric Chemistry and Physics*, *17*(9). https://doi.org/10.5194/acp-17-6073-2017